Tectonophysics 456 (2008) 171–179

Contents lists available at ScienceDirect

Tectonophysics

journal homepage: www.elsevier.com/locate/tecto

Low-temperature thermal evolution of the Azov Massif (Ukrainian Shield–Ukraine) — Implications for interpreting (U–Th)/He and fission track ages from cratons

Martin Danišík [a,*], Reinhard F. Sachsenhofer [b], Vitaliy A. Privalov [c], Elena A. Panova [d], Wolfgang Frisch [a], Cornelia Spiegel [a,e]

[a] *Institute of Geosciences, University of Tübingen, Sigwartstrasse 10, D-72076 Tübingen, Germany*
[b] *Department of Applied Geosciences and Geophysics, University of Leoben, Peter-Tunner-Strasse 5, A-8700, Leoben, Austria*
[c] *Donetsk State Technical University, Artem str., UA-84000 Donetsk, Ukraine*
[d] *UkrNIMI, Tchelyuskintsev str. 291, UA-83121 Donetsk, Ukraine*
[e] *Department of Geosciences, University of Bremen, PO Box 330 440, D-28334 Bremen, Germany*

A R T I C L E I N F O

Article history:
Received 9 January 2008
Received in revised form 18 April 2008
Accepted 19 April 2008
Available online 29 April 2008

Keywords:
Azov Massif
East European Craton
Fission track dating
(U–Th)/He dating
Thermal history modelling
Alpha ejection correction

A B S T R A C T

The low-temperature thermal evolution of the Azov Massif (eastern part of the Ukrainian Shield, Ukraine) is investigated by combined zircon fission track (ZFT), apatite fission track (AFT) and apatite (U–Th)/He (AHe) thermochronology. The data help to better understand the geodynamic evolution of the Azov Massif and the adjacent intra-cratonic rift basin (Dniepr–Donets Basin) as follows:

ZFT data reveal that the Precambrian crystalline basement of the Azov Massif was heated to temperatures close to ~240 °C during the Late Palaeozoic. The heating event is interpreted in terms of burial of the basement beneath a several kilometres thick pile of Devonian and Carboniferous sedimentary deposits of the adjacent Dniepr–Donets Basin. During Permo-Triassic times, large parts of the basement were affected by a thermal event related to mantle upwelling, associated magmatic activity and increased heat flow in the adjacent rift. The major part of the basement cooled to near-surface conditions in the Early to Middle Triassic and since then was thermally stable as suggested by AFT and AHe data. Further, AFT data confirm Late Triassic magmatic activity in the Azov Massif, which, however, did not influence regional thermal pattern. The northern part of the basement and its sedimentary cover record a cooling event in the Jurassic, which was probably related to erosion. However, although Ar–Ar data of Jurassic magmatic activity in the Donbas Foldbelt are about 20 My younger than the AFT data, thermal relaxation after elevated heat flow associated with this magmatic event cannot be completely ruled out.

Our results reveal apparent inconsistencies between AFT and AHe data: the AHe ages corrected for alpha ejection according to the standard procedure [Farley, K.A., Wolf, R.A., Silver, L.T., 1996. The effect of long alpha-stopping distances on (U–Th)/He ages. Geochim. Cosmochim. Acta 60(21), 4223–4229.; Farley, K.A., 2002. (U–Th)/He dating: Techniques, calibrations, and applications. Mineral. Soc. Am. Rev. Mineral. Geochem. 47, 819–844] are older than corresponding AFT ages. In order to test the relevance of alpha ejection correction, mechanical abrasion of several apatite grains was applied. We found that in case of relatively slow cooling, alpha ejection correction of raw (U–Th)/He ages leads to erroneously high ages. This shows that alpha ejection correction should be used with caution. We propose that this correction should only be applied to samples with a fast cooling history, whereas it should not be applied to slowly cooled samples and to samples whose thermal history is not constrained by other means.

1. Introduction

Low-temperature thermochronometers such as fission track and (U–Th)/He dating have been widely used to constrain the exhumation history of cratons and to test their inferred tectonic and thermal stability (e.g., Harman et al., 1998; Reiners and Farley, 2001; Gleadow et al., 2002; Kohn et al., 2002; Osadetz et al., 2002; Belton et al., 2004; Lorencak et al., 2004; Hendriks and Redfield, 2005; Söderlund et al., 2005; Flowers et al., 2006). It was soon recognized that there are often serious discrepancies between apatite fission track (AFT) and apatite (U–Th)/He (AHe) ages. Several studies showed that AHe ages from old, slowly cooled terranes are hardly reproducible (e.g., Fitzgerald et al., 2006). Moreover, AFT ages, which record cooling through the temperature range of ~60–120 °C (e.g., Wagner and Van den haute,

* Corresponding author. Tel.: +49 7071 2974703; fax: +49 7071 5059.
E-mail addresses: martin.danisik@uni-tuebingen.de (M. Danišík), reinhard.sachsenhofer@mu-leoben.at (R.F. Sachsenhofer), vitaliy.privalov@gmail.com (V.A. Privalov), elena.panova@un.org.ua (E.A. Panova), frisch@uni-tuebingen.de (W. Frisch), cornelia.spiegel@uni-bremen.de (C. Spiegel).

0040-1951/$ – see front matter © 2008 Elsevier B.V. All rights reserved.
doi:10.1016/j.tecto.2008.04.022

1992), are often younger than the AHe ages (e.g., Hendriks, 2003; Lorencak, 2003; Belton et al., 2004; Crowhurst et al., 2004; Hendriks and Redfield, 2005; Söderlund et al., 2005; Green et al., 2006), which record cooling through the range of ~40–85 °C (Wolf et al., 1998; Farley, 2000). Therefore, the interpretation of thermochronological data from cratons became a matter of intensive discussion (e.g., Hendriks and Redfield, 2005; Green and Duddy, 2006; Green et al., 2006; Shuster et al., 2006). It is not clear whether the discrepancy arises from not yet fully understood diffusion and retentivity of He, and/or from annealing kinetics of fission tracks in apatites. Some authors suggested that radiation-enhanced annealing in slowly cooled terrains like Scandinavia might lead to 'too young' AFT ages (e.g., Hendriks and Redfield, 2005; Söderlund et al., 2005). Other authors locate the problem in the not yet fully understood mechanisms, which controls diffusion and retentivity of He (Green and Duddy, 2006; Green et al., 2006).

Our study has (1) a regional and (2) a possibly far-reaching methodical aspect:

1) We combine zircon fission track (ZFT), apatite fission track and apatite (U–Th)/He thermochronology to reveal the thermal evolution of the Azov Massif, which represents the eastern part of the Ukrainian Shield. The thermal evolution of this region is actually unconstrained. The low-temperature thermochronological data

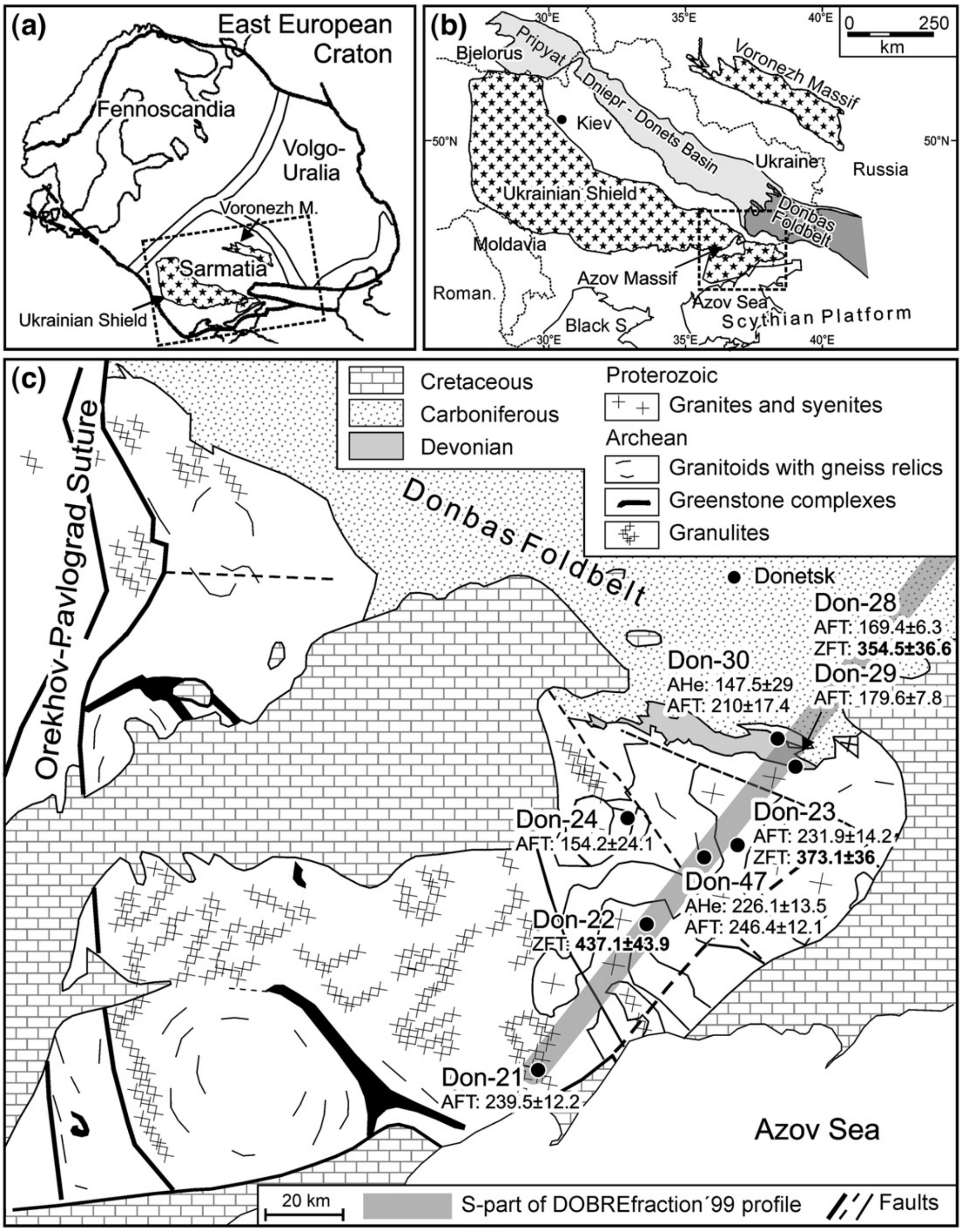

Fig. 1. (a) Tectonic complexes in the East European Craton. (b) Sketch map showing the position of the Ukrainian Shield (including the Azov Massif) and the Voronezh Massif within the southern part of the Eastern European Craton (after Stovba and Stephenson, 1999). (c) Pre-Cenozoic subcrop map of the Azov Massif (after Antsiferov et al., 2004; Kolosovska et al., 2007) together with sample locations and measured ages.

Table 1
ZFT data[a]

Code	Lat/Lon (WGS84)		Petrography	Stratigraphy	N	RhoS	N_s	RhoI	N_i	RhoD	N_d	$P(\chi^2)$ (%)	Age (Ma)	±1σ(Ma)
Don-22	47.301308	37.574556	Syenite	Pre-Cambrian	20	325.18	1250	29.992	115	6.733	3089	N95	437.1	43.9
Don-23	47.456700	37.831365	Syenite	Pre-Cambrian	20	305.41	1174	33.04	127	6.723	3089	N95	373.1	36
Don-28	47.615319	38.008391	Sandstone	Frasnian (380 Ma)	19	266.99	975	30.4	111	6.713	3089	N95	354.5	36.6

[a] N – number of dated zircon crystals; RhoS (RhoI) – spontaneous (induced) track densities (×10^5 tracks/cm^2); N_s (N_i) – number of counted spontaneous (induced) tracks; RhoD – dosimeter track density (×10^5 tracks/cm^2); N_d – number of tracks counted on dosimeter; $P(\chi^2)$ – probability obtaining Chi-square value (χ^2) for n degree of freedom (where n = No. of crystals – 1); Age ± 1σ – central age ± 1 standard error (Galbraith and Laslett , 1993). Ages were calculated using zeta calibration method (Hurford and Green, 1983), glass dosimeter CN-5, and zeta value of 123.6 ± 2.1 year/cm^2.

help to a better understanding of the geodynamic evolution of the Azov Massif and the adjacent intra-cratonic rift basin (Pripyat–Dniepr–Donets Basin; see Stovba and Stephenson, 1999).
2) Our AFT and raw AHe ages are internally consistent unless corrected for alpha ejection (Farley et al., 1996; Farley, 2002). With a simple experiment we try to demonstrate that application of the alpha ejection correction should be applied with caution since it can easily lead to overestimation of true ages and thus to erroneous interpretations.

2. Geological setting

Crystalline rocks of the southern part of the East European Craton (Sarmatia) are exposed in the Ukrainian Shield and the Voronezh Massif (Fig. 1). The two areas are separated by the Late Palaeozoic NW–SE trending Pripyat–Dniepr–Donets rift basin (e.g., Stovba et al., 1996; Stephenson et al., 2001).

The Azov Massif forms the eastern domain of the Ukrainian Shield. It comprises Archean crust, which was reworked in the Palaeoproterozoic (c. 1.8 Ga) and intruded by post-tectonic granites and syenites (Claesson et al., 2006). Towards the north the basement rocks are overlain by Middle Devonian to Lower Carboniferous sediments of the Donbas Foldbelt (DF), which is the inverted part of the Pripyat–Dniepr–Donets Basin (e.g., McCann et al., 2003). Both, Precambrian and Palaeozoic rocks are partly covered by Cretaceous deposits (Stephenson et al., 2004). The crustal thickness of the Azov Massif along the DOBREfraction'99 profile (Fig. 1c) is about 40 km (DOBREfraction'99 Working Group, 2003; Lyngsie et al., 2007).

During Late Devonian rifting the basement was affected by magmatic activity as indicated by Devonian dikes cutting the crystalline basement (Muratov, 1972; Shalatov, 1986). However magmatic activity was not restricted to the syn-rift phase. Early Permian, Middle/Late Triassic and Middle/Late Jurassic ages were obtained for dykes within the Azov Massif (Shalatov, 1986; Alexandre et al., 2004). Indications for a Permo-Triassic heating event in the DF related to magmatic activity were found by Aleksandrov et al. (1996), Sachsenhofer et al. (2002), and Spiegel et al. (2004).

Stovba and Stephenson (1999) presumed that large parts of the currently exposed Azov Massif were covered by Devonian and Carboniferous rocks prior to Permian uplift. This assumption is based on the observation that in the DF progressively older sediments are subcropping beneath the pre-Mesozoic erosion surface in the direction of the Ukrainian Shield. Based on stratigraphic continuity and sediment diagenesis observations, Stovba and Stephenson (1999) supposed that erosion of sediments at the south-eastern margin of the DF was more than 5 km. Although erosion on the Azov Massif was certainly considerable, the magnitude of uplift is purely speculative (Stephenson et al., 2006). Elevated seismic velocities within the present-day Azov crust as compared to that exposed in the Voronezh Massif could be related to major Permian uplift (DOBREfraction'99 Working Group, 2003).

Due to lack of data, the Phanerozoic thermal evolution of the Azov Massif is in fact unconstrained. It is assumed that it was linked to the thermal evolution of the neighbouring DF, which was characterized by a complex thermal history with several Devonian to Cretaceous heating and cooling events (e.g., Sachsenhofer et al., 2002; Spiegel et al., 2004).

3. Samples and methods

For this study, twelve samples were collected for thermochronological investigations, however, three of them did not contain a sufficient amount of datable minerals. The samples were taken from the Precambrian crystalline basement of the Azov Massif and its lower Upper Devonian (Frasnian) sedimentary cover (Tables 1, 2). With the exception of Don-24, sample locations are aligned along the DOBREfraction´99 profile.

Fission track analysis was carried out in the Thermochronological Laboratory of the University of Tübingen (Germany) using standard procedures described in Danišík et al. (2007). We used the external detector method (Gleadow, 1981) with the etching protocols of

Table 2
AFT data[a]

Code	Lat/Lon (WGS84)		Stratigraphy	Petrography	N	RhoS	N_s	RhoI	N_i	RhoD	N_d	$P(\chi^2)$ (%)	Disp.	U (±v.c.)	Age (Ma)	±1σ (Ma)	MTL (µm)	SD (µm)	N (L)	D_{par} (µm)
DON-21	47.301308	37.574556	Pre-Cambrian	Jaspilite	20	82.900	1434	42.895	742	7.825	3736	N95	0	67(±24)	239.5	12.2	13.3	1.0	120	1.7
DON-47	47.433216	37.741547	Pre-Cambrian	Basement	20	15.160	1588	7.742	811	7.949	3736	87.5	0	12(±28)	246.4	12.1	13.2	1.3	100	1.7
DON-23	47.456700	37.831365	Pre-Cambrian	Syenite	20	27.159	890	14.617	479	7.874	3736	N95	0	27(±68)	231.9	14.2	12.5	1.3	101	1.6
DON-24	47.507673	37.534918	Pre-Cambrian (1.75 Ga)	Syenite	65	21.899	2740	18.638	2332	7.924	3736	0	0.29	35(±72)	154.2	8.1				2.2
DON-28	47.615319	38.008391	Frasnian (380 Ma)	Sandstone	36	21.521	2792	16.110	2090	7.961	3675	79.8	0.01	29(±59)	169.4	6.3	13.0	1.2	101	2.1
DON-29	47.617296	38.003118	Frasnian (380 Ma)	Volcanoclastic	23	16.517	1773	11.617	1247	7.936	3736	94.5	0	28(±112)	179.6	7.8	12.6	1.8	108	1.7
DON-30	47.697832	37.846582	Triassic	Andesite	25	4.930	425	2.912	251	7.812	3736	N95	0	6(±94)	210	17.4	13.7	1.4	99	1.7

[a] N – number of dated apatite crystals; RhoS (RhoI) – spontaneous (induced) track densities (×10^5 tracks/cm^2); N_s (N_i) – number of counted spontaneous (induced) tracks; RhoD – dosimeter track density (×10^5 tracks/cm^2); N_d – number of tracks counted on dosimeter; $P(\chi^2)$ – probability obtaining Chi-square value (χ^2) for n degree of freedom (where n = No. of crystals − 1); Disp. – dispersion; U (±v.c.) – average uranium content in ppm and its variation coefficient in %; Age ± 1σ — central age ± 1 standard error (Galbraith and Laslett, 1993); MTL – mean track length; SE – standard error of mean track length; SD – standard deviation of track length distribution; N(L) –number of horizontal confined tracks measured; D_{par} – average etch pit diameter of fission tracks. Ages were calculated using zeta calibration method (Hurford and Green, 1983), glass dosimeter CN-5, and zeta value of 322.7 ± 5.3 year/cm^2.

Table 3
(U–Th)/He data[a]

Sample code	N_c	Th (ng)	Th error (%)	U (ng)	U error (%)	^{4}He (ncc at STP)	^{4}Heerror (%)	TAU (%)	Th/U	Unc. age (Ma)	±1σ (Ma)	F_t	Cor. age (Ma)	±1σ (Ma)	AFT age (Ma)	±1σ (Ma)
DON-30#2	1	0.224	2.7	0.215	2.9	5.315	0.9	2.9	1.04	161.9	4.7	0.87	187.2	10.8	210.0	17.4
DON-30#6	1	0.040	6.2	0.015	6.2	0.353	0.9	6.2	2.66	118.3	7.4	0.80	148.2	11.9		
DON-30#7	1	0.249	2.8	0.078	3.9	2.720	0.9	3.2	3.17	162.1	5.3	0.84	193.0	11.5		
DON-30#9	1	1.256	2.4	0.142	3.4	7.006	0.9	2.7	8.83	131.0	3.5	0.84	155.8	8.8		
DON-30#14	1	0.265	2.2	0.035	3.1	1.424	0.9	2.5	7.66	120.3	3.0	0.79	152.9	8.5		
DON-30#15	1	1.011	10.1	0.018	5.7	0.478	0.9	7.8	0.64	191.3	14.9	0.80	238.5	22.0		
Average (Ma) Std. dev. (Ma)										**147.5**	**29.0**		**179.3**	**34.6**		
DON-47#3	1	0.324	3.1	0.274	3.1	9.381	0.9	3.3	1.19	217.7	7.1	0.83	263.2	15.7	246.4	12.1
DON-47#4	1	0.293	2.4	0.280	1.9	8.948	0.9	2.3	1.05	208.1	4.9	0.83	249.5	13.8		
DON-47#5	1	0.336	2.9	0.225	4.0	9.583	0.9	3.5	1.49	255.2	8.9	0.81	316.2	19.3		
DON-47#6	1	0.259	2.2	0.206	3.5	7.226	0.9	3.0	1.26	220.3	6.6	0.78	283.5	16.5		
DON-47#8	1	0.328	3.2	0.231	3.1	7.586	0.9	3.3	1.42	200.4	6.6	0.83	240.9	14.4		
DON-47#11	1	0.280	2.2	0.251	2.7	9.922	0.9	2.6	1.12	253.5	6.6	0.81	311.8	17.5		
Average (Ma)Std. dev. (Ma)										**225.9**	**23.2**		**277.5**	**31.8**		
Abraded grains																
Don-47R#10x	1	0.085	2.7	0.052	3.2	2.193	0.9	3.0	1.53	248.5	7.6	1	248.5	14.5	246.4	12.1
Don-47R#13x	1	0.036	4.4	0.050	3.2	1.529	0.9	3.9	0.71	211.9	8.2	1	211.9	13.4		
Don-47R#17x	1	0.113	2.5	0.089	2.8	3.074	0.9	2.8	1.19	215.8	6.1	1	215.8	12.4		
Don-47R#19x	1	0.085	3.2	0.064	2.7	2.356	0.9	3.1	1.22	228.8	7.2	1	228.8	13.5		
Don-47R#22x	1	0.102	3.9	0.087	3.6	2.984	0.9	3.9	1.09	218.8	8.5	1	218.8	13.8		
Don-47R#23x	1	0.102	2.7	0.088	3.1	3.223	0.9	3.1	1.08	232.6	7.1	1	232.6	13.6		
Average (Ma) Std. dev. (Ma)													**226.1**	**13.5**		

[a] N_c – number of dated apatite crystals; TAU – total analytical uncertainty; Unc. age – uncorrected AHe age; F_t – alpha recoil correction factor after Farley et al. (1996); Cor. age – corrected AHe age; abraded grains are marked with x.

Donelick et al. (1999) for apatites and of Zaun and Wagner (1985) for zircons. The zeta calibration approach (Hurford and Green, 1983) was adopted to determine the age. The annealing properties of apatite grains were assessed by measurement of Dpar values (Dpar — the mean etch pit diameter of fission tracks on prismatic surfaces of apatite; e.g., Burtner et al., 1994).

For (U–Th)/He analysis, apatite crystals were hand-picked following strict selection criteria as described by Farley (2002), photographed and measured. Selected crystals were degassed under vacuum using laser-heating and analysed for He using a Pfeiffer Prisma QMS-200 mass spectrometer in the Thermochronological Laboratory of the University of Tübingen. Following He measurements, the crystals were analysed by isotope dilution for U and Th at the Scottish Universities Environmental Research Centre (SUERC) in East Kilbride (Scotland) on a VG PlasmaQuad 2 ICP–MS. For more details on analytical procedures the reader is referred to Danišík (2005). The total analytical uncertainty (TAU) was computed as a square root of sum of squares of weighted uncertainties on U, Th, and He measurements. TAU was usually less than ~4% (1 sigma) and was used to calculate the error of raw (U–Th)/He ages. The raw (U–Th)/He ages were corrected for alpha ejection after Farley et al. (1996). The value of 5% was adopted as the uncertainty of Ft correction, and was used to calculate errors of corrected (U–Th)/He ages. Replicate analyses of Durango apatite (59 analyses) over the period of He measurements yielded a mean (U–Th)/He age of 31.7 with a standard deviation of 2 Ma, which is in good agreement with the Durango (U–Th)/He age of 31.13±1.01 Ma reported by McDowell et al. (2005).

The low-temperature thermal history based on AFT data (age, track length and Dpar data) and (U–Th)/He data was modelled using the HeFTy modelling program (Ketcham, 2005). Time–temperature (tT) paths were calculated by the multikinetic annealing model of Ketcham et al. (1999) and diffusion kinetics of the Durango apatite (Farley, 2000).

4. Results and discussion

The results of the FT and (U–Th)/He analyses are summarised in Tables 1, 2 and 3 and shown in Fig. 1c. FT ages are reported as central ages with 1σ errors.

4.1. Zircon fission track data

ZFT analyses were performed on two basement samples (Don-22, 23) and one sample from the sedimentary cover (Don-28; Table 1). The samples yielded ages of 437.1±43.9, 373.1±36, and 354.5±36.6 Ma.

The ZFT age of the sedimentary sample (Don-28) is slightly younger than the depositional age. This indicates that the maximum temperature after deposition was close to ~240 °C and the ZFT system was partially reset. This temperature estimate is also supported by vitrinite reflectance data (N2.5%Rr) from overlying Lower Carboniferous rocks (Levenshtein et al., 1991). Further, the ZFT age coincides with the Late Devonian major rifting phase of the Pripyat–Dniepr–Donets Basin, however the peak temperatures were probably reached during Late Carboniferous/Early Permian maximum burial (e.g. Sachsenhofer et al., 2002).

The ZFT ages of the basement samples are younger than the intrusion ages and in fact similar to the ZFT age of the sedimentary sample. Thus we conclude that during the Late Palaeozoic the basement samples experienced the same thermal evolution with partial resetting of the ZFT system as the sedimentary sample. This conclusion supports the idea of Stovba and Stephenson (1999) that significant parts of the Azov Massif were covered by Late Palaeozoic sediments, several kilometres thick.

4.2. Apatite fission track data

Three basement samples aligned along the DOBREfraction'99 profile (Don-21, 23, 47) revealed a tight cluster of Triassic ages (AFT ages: 246.4±12.1, 239.5±12.2, 231.9.±14.2 Ma). Track length distributions (Fig. 2) are unimodal, with mean track lengths (MTL) of 12.5 to 13.3 μm and standard deviations (SD) of 1 to 1.3 μm. These values are typical of rocks with slow cooling through the apatite partial annealing zone (APAZ; e.g., Gleadow et al., 1986a,b). The modelled thermal histories of the samples revealed fairly similar tT paths with cooling through the APAZ to near-surface conditions during the Triassic (Fig. 3a). We conclude that the eastern part of the Azov Massif became thermally stable since that time. It is likely that this cooling episode was related to the termination of a Permo-Triassic thermal event associated with andesitic magmatism and high heat flow. This

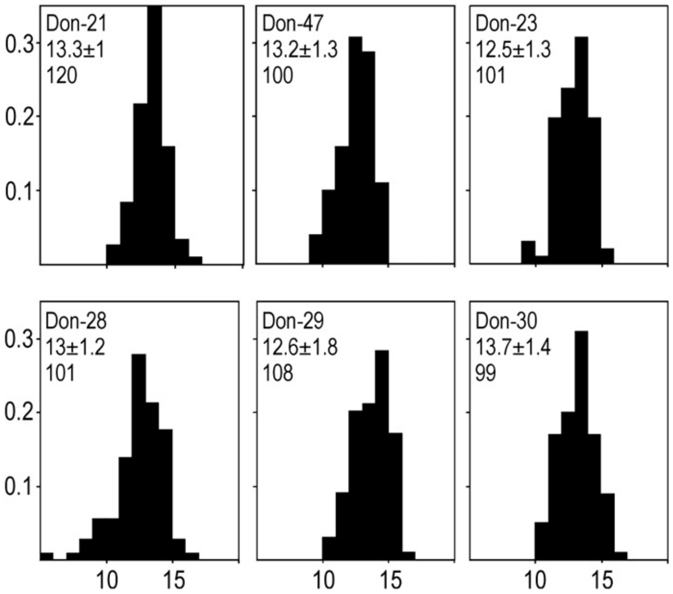

Fig. 2. Confined track length distributions of measured samples. Explanation of histograms: *y*-axis: frequency of tracks; *x*-axis: length in μm; text from the top: sample code; mean track length ± standard deviation (both in μm); number of measured tracks.

event was first predicted by modelling of vitrinite reflectance (VR) data (Sachsenhofer et al., 2002) and later confirmed by FT data from the DF (Spiegel et al., 2004). Moreover, Spiegel et al. (2004) correctly envisaged that the Permo-Triassic thermal event had regional character and affected a broad area including parts of the East European Craton.

The basement sample Don-24 yielded the age of 166 ± 12.9 Ma. However, this sample failed the chi-square test and shows high dispersion (0.29), which indicates broad single grain age distribution. Therefore, we tried to recognize individual age components on the basis of Dpar measurements and using the PopShare software (Dunkl and Székely, 2003). We found a positive correlation between single grain ages and Dpar values and identified three age populations: 88 ± 10 Ma with Dpar ~ 1.6 μm, 160 ± 30 Ma with Dpar ~ 2 μm, and a weakly constrained population of 251 ± 50 Ma with Dpar ~ 3.3 μm (Fig. 4). We interpret the oldest age group (251 ± 50 Ma), which is formed by more annealing resistant apatites, to record the same cooling event as the other basement samples. The two younger age populations are formed by less-annealing resistant grains, as indicated by the Dpar values, and are therefore sensitive to slightly lower temperatures. These age populations indicate that this part of the basement experienced final cooling during Jurassic–Cretaceous times, which, however, must be confirmed by more data. Nevertheless, this preliminary interpretation is in accord with conclusions of Spiegel et al. (2004). From AFT and vitrinite reflectance numerical modelling results they argued that the Donets region was thermally active in Jurassic and possibly Cretaceous times. Both samples (Don-28, 29) from the Frasnian sedimentary cover passed the chi-square test and yielded central AFT ages of 179.6 ± 7.8 and 169.4 ± 6.3 Ma that are much younger than their depositional age (~ 380 Ma), implying reheating to temperatures above ~ 100 °C. Track length distributions (Fig. 2) are unimodal, with MTL's of 12.6 and 13 μm and standard deviations of 1.2 and 1.8 μm. The thermal evolution between Devonian temperatures recorded by the ZFT age and onset of final cooling cannot be revealed by thermal modelling (Fig. 3c). Nevertheless, an important conclusion drawn from the modelled tT paths is that final cooling of both samples occurred in the Jurassic. Cooling after a Jurassic thermal event related to elevated heat flows associated with magmatic activity in the DFB would be an obvious explanation. However, the magmatic event (~ 155 Ma; Lazarenko et al., 1975; Alexandre et al., 2004) post-dates the observed AFT ages. Thus, the cooling ages may indicate Jurassic exhumation (see also Spiegel et al., 2004), which might be related to a mid-Jurassic compressional event affecting the southern margin of the East European Craton (Saintot et al., 2006).

Sample Don-30, taken from an andesite dyke revealed an AFT age of 210 ± 17.4 Ma and unimodal track length distribution with MTL of 13.7 μm and SD of 1.4 μm (Fig. 2). The same dyke has been dated by Alexandre et al. (2004; their sample UK07) by Ar–Ar on amphibole, yielding an age of 226 ± 34.7 Ma. Similar dykes from other localities (close to site Don-28/29) yielded ages of 214.3 ± 12.7 and 214.3 ± 14.2 Ma, respectively (Alexandre et al., 2004). Slight difference between Ar–Ar and AFT ages together with minor shortening of the tracks indicate fast cooling of the dyke after emplacement and confirms Late Triassic magmatic activity in the Azov Massif.

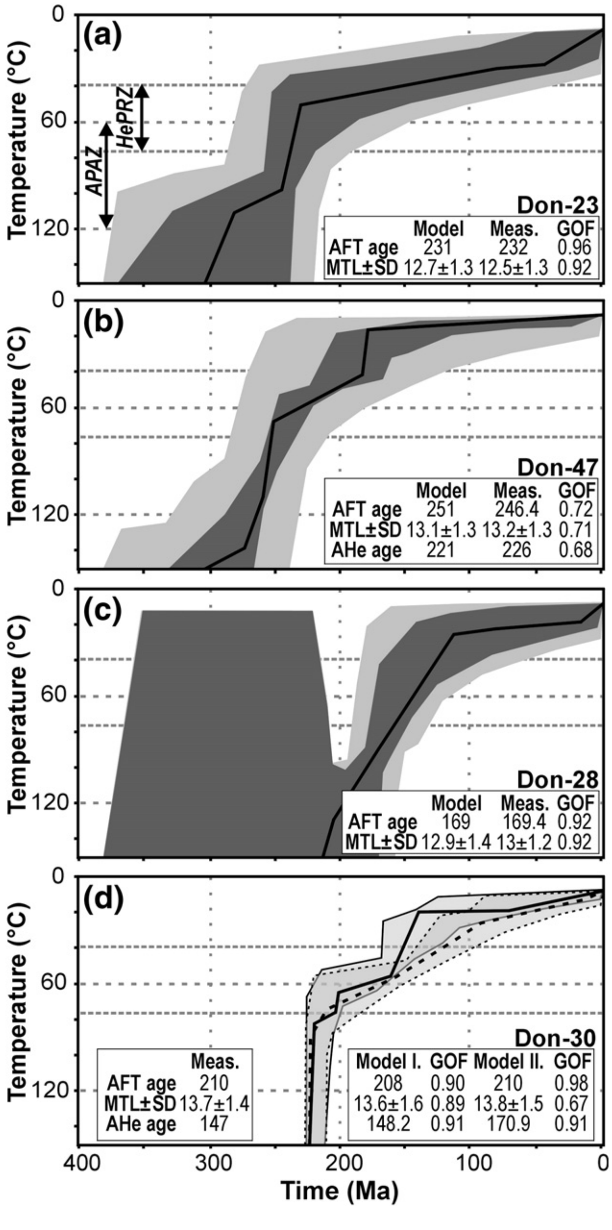

Fig. 3. Thermal modelling results of AFT and AHe data displayed in time–temperature diagrams modelled with HeFTy program (Ketcham, 2005). Light grey envelopes indicate acceptable fit; dark grey envelopes indicate good fit; Thick lines indicate the best fit; APAZ-apatite partial annealing zone; HePRZ-apatite helium partial retention zone; MTL is mean track length in μm; SD is standard deviation in μm; GOF is goodness of fit (statistical comparison of the measured input data and modelled output data, where a "good" result corresponds to value 0.5 or higher, "the best" result corresponds to value 1). The last panel depicts good and best fits for the sample Don-30 based on raw (dashed lines) and corrected AHe age (solid lines).

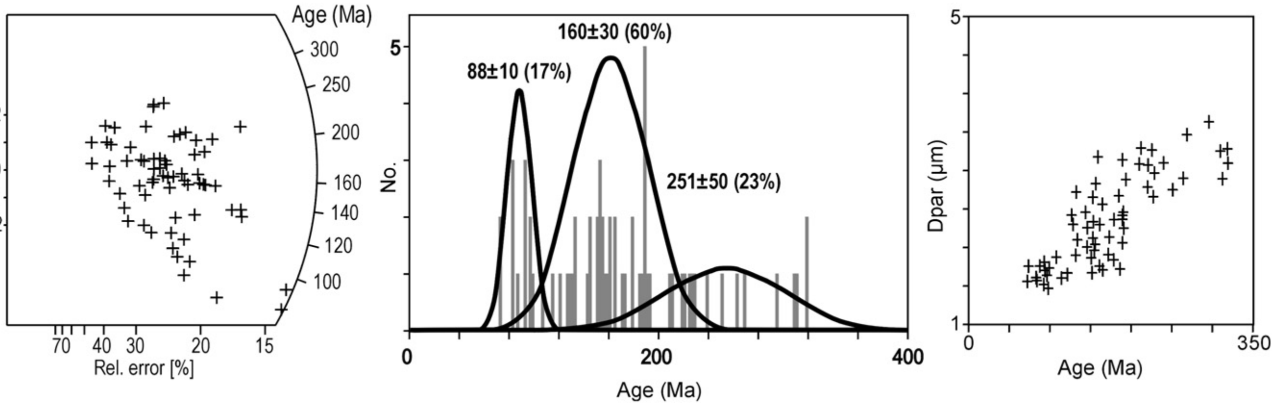

Fig. 4. Radial plot, histogram of single grain ages with identified age groups and AFT age vs. Dpar plot of the sample Don-24.

In summary, our FT data show so far that (1) the Azov Massif experienced temperatures close to ~240 °C in the Late Palaeozoic, (2) it was further affected by a Permo-Triassic thermal event, in agreement with independent geological constraints regarding the magmatic and erosional evolution of the DF, and (3) the northern margin of the Azov Massif remained tectonically more or less quiet since the late Triassic. Therefore, we expect AHe ages from the Azov Massif that are consistent with the geological history and the other thermochronological data of that area to be Triassic or younger.

4.3. (U–Th)/He data

For (U–Th)/He analysis, only two samples (Don-30, Don-47) contained sufficient amount of suitable apatite crystals with respect to morphology and purity that is critically important for successful (U–Th)/He dating.

From sample Don-47, 6 apatite grains were analysed, yielding corrected AHe ages between 240.9±14.4 to 316.2±19.3 Ma with an average of 277.5±31.8 Ma, which is clearly higher than and thus inconsistent with the corresponding AFT age (246.4±12.1 Ma).

Similar observations were reported by several studies (e.g., Hendriks, 2003; Lorencak, 2003; Belton et al., 2004; Crowhurst et al., 2004; Hendriks and Redfield, 2005; Green et al., 2006), and explanations such as slow cooling (Fitzgerald et al., 2006) and zoning of Uranium and/or Thorium (Meesters and Dunai, 2002a,b) have been proposed. Currently most preferred explanation was first foreseen by Farley (2000) and Crowley et al. (2002), and later elaborated by Shuster et al. (2006). Shuster et al. (2006) reasonably explained the phenomenon of 'too old' AHe ages by accumulation of radiation damage in the crystal structure of apatite, which increase the retentivity of He and thus closure temperature of (U–Th)/He system in apatite by up to ±15 °C. Green et al. (2006) demonstrated that 'too old' AHe ages are to be expected in apatites with Uranium content above ~10 ppm with FT age of more than ~100 Ma, which applies to the sample Don-47 (AFT age: 246.4±12.1 Ma, Uranium: ~12 ppm; Table 2). There are, however, some exceptions that do not follow this 'general guide' (see e.g., Hansen and Reiners, 2006).

We fully acknowledge the advances achieved in this problem, but on the example of the sample Don-47 we like to propose an alternative explanation, which involves routinely used alpha ejection correction (Ft correction; Farley et al., 1996; Farley, 2002). As mentioned above, 6 replicates of the sample Don-47 yielded AHe ages between 240.9±14.4 to 316.2±19.3 Ma with an average of 277.5±31.8 Ma, that is higher than the corresponding AFT age (246.4±12.1 Ma). If however the alpha ejection correction is not applied, the AHe ages decrease to 200.4±6.6 to 255.2±8.9 Ma with an average AHe age of 225.9±23.2 Ma, which is slightly lower than and thus consistent with the AFT age. The question arising at this point is, whether the application of alpha ejection correction is relevant? In order to address this issue, we hand-picked another set of apatites from the sample Don-47 and mechanically abraded their outermost rim of ~30 µm. By doing so, we aimed to remove the 'skin' of the crystals, which is affected by ejection/implantation of alpha particles that have stopping distance from 12.6 to 34.1 µm averaged at ~20 µm in apatite (Ziegler, 1977; Farley et al., 1996; Farley, 2002). The advantage of this approach is that raw AHe ages do not need to be corrected for alpha ejection (Ft factor=1). This approach was recommended by Farley et al. (1996), but the authors emphasized that it can be applied to crystals with homogeneous distribution of parent nuclides, but can be problematic for zoned grains. In contrast, Farley (2002) pointed out that removal of outermost rim can bias the age of remaining crystal towards erroneously high values, because He in the grain can be depleted not only due to alpha ejection but also due to diffusion of He that is controlled by the crystal's thermal history.

Uranium distribution in the apatites of sample Don-47 was homogenous as inferred from fission track mounts, distribution of Th was not determined but was assumed to be homogeneous. A total of 6 abraded apatite grains were analysed by the (U–Th)/He method. The grains yielded AHe ages between 211.9±8.2 and 248.5±7.6 Ma with an average of 226.1±13.5 Ma (Table 3), which are practically identical values as revealed by raw (uncorrected) AHe ages of non-abraded grains (Fig. 5). This in our opinion clearly shows that at least in the case of this sample, alpha ejection correction led to erroneous overcorrection of true AHe ages.

Possible reason for this can be explained as follows: despite being currently customary used in almost all (U–Th)/He studies, Ft

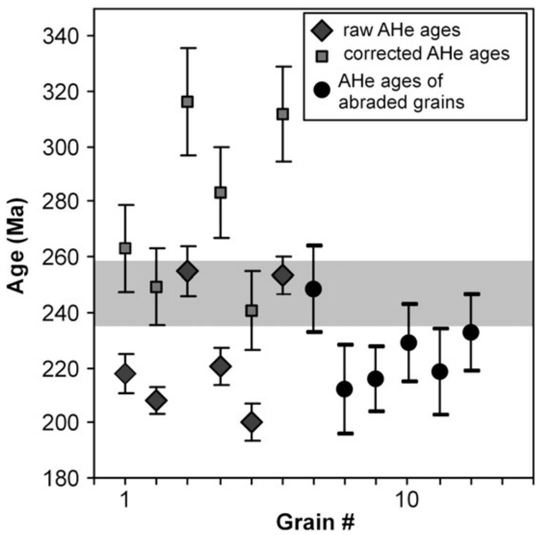

Fig. 5. Diagram of AHe ages from non-abraded (squares) and abraded (dots) apatite grains. Grey band indicates AFT age of the sample.

correction is evidently a simplification and has some drawbacks (Farley et al., 1996; Farley, 2002): it (i) assumes homogeneous distribution of parent isotopes in the dated crystals, (ii) assumes no implantation of helium from surrounding matrix and, most importantly, (iii) neglects diffusion. In our opinion, the first two points do not apply to the sample Don-47, since, as mentioned above, we did not observe any zonation of U and did not find any minerals that would indicate a 'bad neighbourhood' capable of alpha-injection into dated apatite grains. Thus, the problem with overcorrected ages can be attributed to diffusion. Meesters and Dunai (2002a,b) by using numerical methods showed that in the absence of diffusion, i.e. when a sample cooled fast through the PRZ, He in the outer parts of the crystal will be depleted due to alpha ejections, thus, for such cases the Ft correction is reasonable. However, if diffusion is important, i.e. if a sample remained a significant period within the PRZ, the crystal will become depleted in He due to diffusive loss, which in turn decreases the amount of ejected He. Consequently, conventional application of Ft correction will generally lead to erroneous overcorrection of AHe ages. This seems to be the case of the sample Don-47. As indicated by track length distribution, cooling could not have been fast and diffusion must have played a role for He retention. Therefore, for thermal history modelling we used uncorrected AHe ages and easily found solutions reconciling both AFT and (U–Th)/He data and being consistent with the independently constrained geological record. Modelled tT paths (Fig. 3b) suggest that the sample reached near-surface conditions already in the Early to Middle Triassic and since then became thermally stable.

By contrast, 6 apatite grains from the sample Don-30 (andesite dike, AFT age 210±17.4 Ma) yielded raw AHe ages between 118.3±7.4 and 191.3±14.9 Ma with an average of 147.5±29 Ma that is much less than the according AFT age, so despite of the relatively high scatter there is no reason to expel the ages from the dataset. After applying the alpha ejection correction, the AHe ages increased to the range of 148.2±11.9 to 238.5±22 Ma with an average of 179.3±34.6 Ma, which is still less than the AFT age, although one grain (Don-30#15: 238.5±22 Ma) became older. Unfortunately, due to lack of suitable apatite grains, the abrasion experiment could not be performed and at this point, one can only speculate whether the Ft correction should be applied or not. Since the AFT and AHe data are not discrepant, it is possible to model thermal trajectories reconciling both raw and corrected AHe ages (Fig. 3d). The modelled tT paths look then slightly different and would of course have different meaning for further geodynamic interpretation. If a rapid cooling scenario justifying Ft correction is assumed, the modelled tT paths based on corrected AHe ages will suggest that the sample reached near-surface conditions already during Late Jurassic times. This scenario can be supported by high cooling rates inferred from Ar–Ar and AFT ages (see above) if the closure temperature concept is assumed (Dodson, 1973). In contrast, if the cooling rate was not that high and the sample remained within the PRZ for a significantly long time, Ft correction cannot be applied and modelled tT paths constrained by raw AHe ages will suggests the final cooling only during mid-Cretaceous times. This scenario is supported by: (i) track length distribution with the MTL of 13.7 µm and SD of 1.4 µm that is slightly less than what is typical for fastly cooled samples (Gleadow et al., 1986a,b); (ii) scatter of single grain AHe ages that is typical for slowly cooled samples (Fitzgerald et al., 2006). We would like to emphasize that all grains selected for (U–Th)/He analysis fulfilled strict selection criteria, and we did not find any correlation between AHe ages, grain size or measured elements content that would account for the observed scatter. Therefore, the only conclusion we can draw so far is that the sample Don-30 cooled to near-surface conditions after the Middle Jurassic.

The two examples presented here may have an impact on presentation and interpretation of (U–Th)/He data: there are several published studies, whose interpretations are based purely on conventionally corrected (U–Th)/He ages, although there is no information on thermal evolution of the dated samples and fast cooling is often simply assumed without any proof for it. The difference between raw and (over)corrected ages is probably most obvious in the samples from old terranes (Palaeozoic and Pre-Cambrian), where the deviation easily exceeds 100 Ma (e.g., Lorencak et al., 2004; Flowers et al., 2006), which is not trivial for correct interpretation at geological time scale. Thus, we suggest that for such samples classical Ft correction should not be applied unless fast cooling of these samples is proven.

5. Conclusions

The first FT and (U–Th)/He data from the Ukrainian Shield enabled us to constrain the thermotectonic evolution of the Azov Massif and its border with the DF. The most important results are summarized as follows (see also Fig. 6):

- The Precambrian crystalline basement of the Azov Massif was heated to temperatures close to ~240 °C in the Late Palaeozoic, as recorded by ZFT data. Heating was induced by burial beneath (Upper Devonian and) Carboniferous rocks several kilometres thick. This indicates that large parts of the Azov Massif were covered by post-rift deposits of the Dniepr–Donets Basin;
- Large parts of the basement were affected by a Permo-Triassic thermal event related to mantle upwelling associated with magmatic activity and increased heat flow. The Permo-Triassic thermal event was not restricted to the DF only but had regional character;
- AFT age from an andesite dike confirms magmatic activity in the Azov Massif during Late Triassic times. This magmatic activity had no effect on regional thermal patterns;
- The major part of the basement cooled to near-surface conditions in the Early to Middle Triassic and since then was thermally stable as suggested by AFT and AHe data;
- In addition to the Permo-Triassic thermal event, the northern part of the basement and its sedimentary cover record a cooling event in the Jurassic. Probably this event is related to erosion. However, although Ar–Ar data of a Jurassic magmatic activity in the DF are about 20 Ma younger than the AFT data, thermal relaxation after elevated heat flow associated with the Jurassic magmatic activity cannot be ruled out completely.

Further, we demonstrated that application of alpha ejection correction to the raw AHe ages of samples from slowly cooled terranes is not straightforward. We suggest that customary used alpha ejection correction (Ft correction) of raw (U–Th)/He ages should be applied only to samples with fast passage through the PRZ. We suggest not to apply this correction to samples with long passage through the PRZ and to samples whose thermal history is not constrained by other

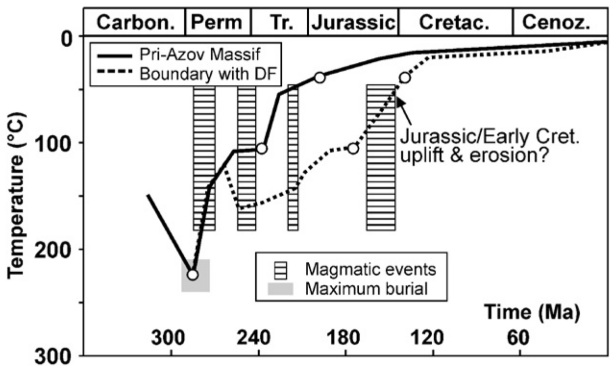

Fig. 6. Sketch summarizing the thermal evolution of the Azov Massif and its border with the Donbas Foldbelt. Note that cooling of the northern border of the Azov Massif significantly post-dates cooling in its central part. Magmatic events after Shalatov (1986) and Alexandre et al. (2004).

means. Otherwise, Ft correction can lead to massive overestimation of true ages.

Acknowledgements

This study was funded by the German Science Foundation (DFG, Project number SP 673/3-1). RFS acknowledges support from a MOEL+ scholarship of the "Österreichische Forschungsgemeinschaft". Sampling was supported by V.A. Antsiferov and A.V. Antsiferov (UkrNIMI, Donetsk). Gerlinde Höckh, Dorothea Mühlbayer-Renner and Dagmar Kost (Tübingen) are thanked for their careful sample preparation. Support by Alexander Kitchka (Kiev) is highly appreciated. An earlier version of the manuscript benefited from the constructive reviews by Paul Green and an anonymous reviewer.

References

Aleksandrov, A.L., Gordienko, V.V., Derevskaya, K.I., Zemskov, G.A., Ivanov, A.P., Panov, B.S., Shumlyanskiy, V.A., Epov, O.G., 1996. Deep structure, evolution of fluid systems and endogenic gold-bearing potentiality, South-Eastern part of Ukrainian Donets Basin (in Russian). Edition of Institute of Fundamental Researches of Ukrainian Scientific Association, Kyiv. 74 pp.

Alexandre, P., Chalot-Prat, F., Saintot, A., Wijbrans, J., Stephenson, R., Wilson, M., Kitchka, A., Stovba, S., 2004. The $^{40}Ar/^{39}Ar$ dating of magmatic activity in the Donbas Fold Belt and the Scythian Platform (Eastern European Craton). Tectonics 23, TC5002.

Antsiferov, A.V., Sheremet, E.M., Glevasskiy, E.B., Esiptchuk, K.E., Nikolayev, Yu.I., Nikolayev, I.Yu., Sukhoy, V.V., 2004. Geological and geophysical model of the Orekhov–Pavlograd Suture zone within the Ukrainian Shield (in Russian). Rock Geology, Rock mechanics and Mine Surveying. Proceedings of the International Science and Technology Conference devoted to the 75th Anniversary of UkrNIMI. National Academy of Science of Ukraine, Donetsk, pp. 54–62.

Belton, D.X., Brown, R.W., Kohn, B.P., Fink, D., Farley, K.A., 2004. Quantitative resolution of the debate over antiquity of the central Australian landscape: implications for the tectonic and geomorphic stability of cratonic interiors. Earth Planet. Sci. Lett. 219, 21–34.

Burtner, R.L., Nigrini, A., Donelick, R.A., 1994. Thermochronology of Lower Cretaceous source rocks in the Idaho–Wyoming thrust belt. AAPG Bull. 78 (10), 1613–1636.

Claesson, S., Bibikova, E., Bogdanova, S., Skobelev, V., 2006. Archean terranes, Paleoproterozoic reworking and accretion in the Ukrainian Shield, East European Craton. In: Gee, D.G., Stephenson, R.A. (Eds.), European Lithosphere Dynamics. Geological Society, London, Memoirs, vol. 32, pp. 645–654.

Crowhurst, P.V., Green, P.F., Farley, K.A., Jacobs, J., Griffin, B., 2004. Anomalously 'old' He ages: what causes them and what can we do about them? (Abstract), 10th International Conference on fission track dating and thermochronology, Amsterdam.

Crowley, P.D., Reiners, P.W., Reuter, J.M., Kaye, G.D., 2002. Laramide exhumation of the Bighorn Mountains, Wyoming: an apatite (U-Th)/He thermochronology study. Geology 30, 27–30.

Danišík, M., 2005. Cooling history and relief evolution of Corsica (France) as constrained by fission track and (U–Th)/He thermochronology, Ph.D. thesis, University of Tübingen, Tübingen, Germany, 130 pp.

Danišík, M., Kuhlemann, j., Dunkl, I., Székely, B., Frisch, W., 2007. Burial and exhumation of Corsica (France) in the light of fission track data. Tectonics 26, TC1001. doi:10.1029/2005TC001938.

DOBREfraction'99 Working GroupGrad, M., Gryn, D., Guterch, A., Janik, T., Keller, R., Lang, R., Lyngsie, S.B., Omelchenko, V., Starostenko, V.I., Stephenson, R.A., Stovba, S.M., Thybo, H., Tolkunov, A., 2003. "DOBREfraction'99" — velocity model of the crust and upper mantle beneath the Donbas Foldbelt (East Ukraine). Tectonophysics 371, 81–110.

Dodson, M.H., 1973. Closure temperature in cooling geochronological and petrological systems. Contrib. Mineral. Petrol. 40, 259–274.

Donelick, R.A., Ketcham, R.A., Carlson, W.D., 1999. Variability of apatite fission-track annealing kinetics: II. Crystallographic orientation effects. Am. Mineral. 84 (9), 1224–1234.

Dunkl, I., Székely, B., 2003. Component analysis with visualization of fitting — PopShare, a freeware program for evaluation of mixed geochronological data. Geophys. Res. Abstr. 5, 02657.

Farley, K.A., 2000. Helium diffusion from apatite: general behavior as illustrated by Durango fluorapatite. J. Geophys. Res. 105 (B2), 2903–2914.

Farley, K.A., 2002. (U–Th)/He dating: techniques, calibrations, and applications. Mineral. Soc. Am. Rev. Mineral. Geochem. 47, 819–844.

Farley, K.A., Wolf, R.A., Silver, L.T., 1996. The effect of long alpha-stopping distances on (U–Th)/He ages. Geochim. Cosmochim. Acta 60 (21), 4223–4229.

Fitzgerald, P.G., Baldwin, S.L., Webb, L.E., O'Sullivan, P.B., 2006. Interpretation of (U–Th)/He single grain ages from slowly cooled crustal terranes: a case study from the Transantarctic Mountains of southern Victoria Land. Chem. Geol. 225, 91–120. doi:10.1016/j.chemgeo.2005.09.001.

Flowers, R.M., Bowring, S.A., Reiners, P.W., 2006. Low long-term erosion rates and extreme continental stability documented by ancient (U–Th)/He dates. Geology 34 (11), 925–928. doi:10.1130/G22670A.1.

Galbraith, R.F., Laslett, G.M., 1993. Statistical models for mixed fission track ages. Nucl. Tracks Radiat. Meas. 21, 459–470.

Gleadow, A.J.W., 1981. Fission track dating methods: what are the real alternatives? Nucl. Tracks Radiat. Meas. 5, 3–14.

Gleadow, A.J.W., Duddy, I.R., Green, P.F., 1986a. Fission track lengths in the apatite annealing zone and the interpretation of mixed ages. Earth Planet. Sci. Lett. 78, 245–254.

Gleadow, A.J.W., Duddy, I.R., Green, P.F., 1986b. Confined fission track lengths in apatite: a diagnostic tool for thermal history analysis. Contrib. Mineral. Petrol. 94, 405–415.

Gleadow, A.J.W., Kohn, B.P., Brown, R.W., O'Sullivan, P.B., Raza, A., 2002. Fission track thermotectonic imaging of the Australian continent. Tectonophysics 349, 5–21. doi:10.1016/S0040-1951(02)00043-4.

Green, P.F., Duddy, I.R., 2006. Interpretation of apatite (U–Th)/He ages and fission track ages from cratons. Earth Planet. Sci. Lett. 244 (3–4), 541–547.

Green, P.F., Crowhurst, P.V., Duddy, I.R., Japsen, P., Holford, S.P., 2006. Conflicting (U–Th)/He and fission track ages in apatite: enhanced He retention, not anomalous annealing behaviour. Earth Planet. Sci. Lett. 250 (3–4), 407–427.

Hansen, K., Reiners, P.W., 2006. Low temperature thermochronology of the southern East Greenland continental margin: evidence from apatite (U-Th)/He and fission track analysis and implications for intermethod calibration. Lithos 92, 117–136.

Harman, R., Gallagher, K., Brown, R., Raza, A., Bizzi, L., 1998. Accelerated denudation and tectonic/geomorphic reactivation of the cratons of northeastern Brazil during the Late Cretaceous. J. Geophys. Res. 103, 27091–27105. doi:10.1029/98JB02524.

Hendriks, B., 2003. Cooling and denudation of the Norwegian and Barents Sea margins, Northern Scandinavia. Constrained by apatite fission track and (U-Th)/He thermochronometry. PhD thesis, Vrije Universiteit, Amsterdam, The Netherlands, 177 pp.

Hendriks, B.W.H., Redfield, T.F., 2005. Apatite fission track and (U–Th)/He data from Fennoscandia: an example of underestimation of fission track annealing in apatite. Earth Planet. Sci. Lett. 236, 443–458.

Hurford, A.J., Green, P.F., 1983. The zeta age calibration of fission-track dating. Chem. Geol. 41, 285–312.

Ketcham, R.A., 2005. Forward and inverse modeling of low-temperature thermochronometry data. In: Reiners, P.W., Ehlers, T.A. (Eds.), Low-Temperature Thermochronology: Techniques, Interpretations, and Applications. Reviews in Mineralogy and Geochemistry, vol. 58, pp. 275–314.

Ketcham, R.A., Donelick, R.A., Carlson, W.D., 1999. Variability of apatite fission-track annealing kinetics: III. Extrapolation to geologic time scales. Am. Mineral. 84, 1235–1255.

Kohn, B.P., Gleadow, A.J.W., Brown, R.W., Gallagher, K., O'Sullivan, P.B., Foster, D.A., 2002. Shaping the Australian crust over the last 300 million years: Insights from fission track thermotectonic imaging and denudation studies of key terranes. Aust. J. Earth Sci. 49, 697–717. doi:10.1046/j.1440-0952.2002.00942.x.

Kolosovska, V.A., Marakhovska, I.I., Demekhin, L.O., Met al.idi, G.M., Sydorova, D.A., Solovytsky, V.M., 2007. Geological Map Pre-Cenozoic Formations of Ukraine. Scale 1:1000 000. State Geological Service of Ukraine.

Lazarenko, E.K., Panov, B.S., Gruba, V.I., 1975. The mineralogy of the Donets Basin, 1 (in Russian). Naukova dumka, Kiev. 225 pp.

Levenshtein, M.L., Spirina, O.I., Nosova, K.B., Dedov, V.S., 1991. Map of coal Metamorphism in the Donetsk Basin (Paleozoic surface). 1:500.000. Ministry of Geology of the USSR, Kiev.

Lorencak, M., 2003. Low temperature thermochronology of the Canadian and Fennoscandian Shields. PhD thesis, University of Melbourne, Melbourne, Australia, 300 pp.

Lorencak, M., Kohn, B.P., Osadetz, K.G., Gleadow, A.J.W., 2004. Combined apatite fission track and (U–Th)/He thermochronometry in a slowly cooled terrane: results from a 3440-m deep drill hole in the southern Canadian shield. Earth Planet. Sci. Lett. 227, 87–104. doi:10.1016/j.epsl.2004.08.015.

Lyngsie, S.B., Thybo, H., Lang, R., 2007. Rifting and lower crustal reflectivity: a case study of the intracratonic Dniepr–Donets rift zone, Ukraine. J. Geophys. Res. 112, B12402. doi:10.1029/2006JB004795.

McCann, T., Saintot, A., Chalot-Prat, F., Kitchka, A., Fokin, P., Alekseev, A., EUROPROBE-INTAS RESEARCH TEAM, 2003. Evolution of the southern margin of the Donbas (Ukraine) from Devonian to Early Carboniferous times. In: McCann, T., Saintot, A. (Eds.), Tracing Tectonic Deformation Using the Sedimentary Record. Geological Society of London, Special Publication, vol. 208, pp. 117–135.

McDowell, F.W., McIntosh, W.C., Farley, K.A., 2005. A precise ^{40}Ar–^{39}Ar reference age for the Durango apatite (U–Th)/He and fission-track dating standard. Chem. Geol. 214, 249–263.

Meesters, A.G.C.A., Dunai, T.J., 2002a. Solving the production–diffusion equation for finite diffusion domains of the various shapes, part 1; implications for low temperature (U–Th) /He thermochronology. Chem. Geol. 186 (3–4), 333–344.

Meesters, A.G.C.A., Dunai, T.J., 2002b. Solving the production–diffusion equation for finite diffusion domains of various shapes part 2, Application to cases with Alpha ejection and non-homogeneous distribution of the source. Chem. Geol. 186 (3–4), 345–363.

Muratov, M.V., 1972. The history of the Black Sea depression comparing to the Mediterranean Sea depressions. Geotectonics 5, 22–41.

Osadetz, K.G., Kohn, B.P., Feinstein, S., O'Sullivan, P.B., 2002. Thermal history of the Williston basin from apatite fission-track thermochronology — implications for petroleum systems and geodynamic history. Tectonophysics 349, 221–249. doi:10.1016/S0040-1951(02)00055-0.

Reiners, P.W., Farley, K.A., 2001. Influence of crystal size on apatite (U–Th)/He thermochronology: an example from the Bighorn Mountains, Wyoming. Earth Planet. Sci. Lett. 188, 413–420. doi:10.1016/S0012-821X(01)00341-7.

Sachsenhofer, R.F., Privalov, V.A., Zhykalyak, M.V., Bueker, C., Panova, E.A., Rainer, T., Shymanovskyy, V.A., Stephenson, R.A., 2002. The Donets Basin (Ukraine/Russia): coalification and thermal history. Int. J. Coal Geol. 49, 33–55.

Saintot, A., Stephenson, R.A., Stovba, S.M., Brunet, M.-F., Yegorova, T., Starostenko, V., 2006. The evolution of the southern margin of Eastern Europe (Eastern European and Scythian platforms) from the latest Precambrian–Early Paleozoic to the Early Cretaceous. In: Gee, D.G., Stephenson, R.A. (Eds.), European Lithosphere Dynamics. Geological Society, London, Memoirs, vol. 32, pp. 481–505.

Shalatov, N., 1986. Dykes of the Priazovie (in Russian). IGS publication Naukova Dumka, Kiev, Ukraine. 192 pp.

Shuster, D.L., Flowers, R.M., Farley, K.A., 2006. The influence of natural radiation damage on helium diffusion kinetics in apatite. Earth Planet. Sci. Lett. 249 (3–4), 148–161.

Söderlund, P., Juez-Larré, J., Page, L.M., Dunai, T.J., 2005. Extending the time range of apatite (U–Th)/He thermochronometry in slowly cooled terranes: Palaeozoic to Cenozoic exhumation history of southeast Sweden. Earth Planet. Sci. Lett. 239, 266–275. doi:10.1016/j.epsl.2005.09.009.

Spiegel, C., Sachsenhofer, R.F., Privalov, V.A., Zhykalyak, M.V., Panova, E.A., 2004. Thermotectonic evolution of the Ukrainian Donbas Foldbelt: evidence from zircon and apatite fission track data. Tectonophysics 383, 193–215.

Stephenson, R.A., Stovba, S.M., Starostenko, V.I., 2001. Pripyat–Dniepr–Donets Basin: implications for dynamics of rifting and the tectonic history of the northern Peri-Tethyan platform. In: Ziegler, P.A., Cavazza, W., Robertson, A.H.F., Crasquin-Soleau, S. (Eds.), Peri-Tethyan Rift/Wrench Basins and Passive Margins, Peri-Tethys Memoir 6. Mémoires du Muséum National d´Histoire Naturelle, vol. 186, pp. 369–406.

Stephenson, R.A., Mart, Y., Okay, A., Robertson, A.H.F., Saintot, A., Stovba, S., Khriachtchevskaia, O., 2004. TRANSMED Transect VIII: Eastern European Craton–Crimea–Black Sea–Anatolia–Cyprus–Levant Sea–Sinai–Red Sea. In: Cavazza, W., Roure, F., Spakman, W., Stampfli, G.M., Ziegler, P.A. (Eds.), The TRANSMED atlas. The Mediterranean region from crust to mantle; geological and geophysical framework of the Mediterranean and the surrounding areas. A publication of the Mediterranean Consortium for the 32nd International Geological Congress. Springer, Berlin. 141 pp.

Stephenson, R.A., Yegorova, T., Brunet, M.-F., Stovba, S., Wilson, M., Starostenko, V., Saintot, A., Kusznier, N., 2006. Late Paleozoic intra- and pericratonic basins on the East European Craton and its margins. In: Gee, D.G., Stephenson, R.A. (Eds.), European Lithosphere Dynamics. Geological Society, London, Memoirs, vol. 32, pp. 463–479.

Stovba, S.M., Stephenson, R.A., Kivshik, M., 1996. Structural features and evolution of the Dniepr-Donets Basin, Ukraine, from regional seismic reflection profiles. Tectonophysics 268, 127–147.

Stovba, S.M., Stephenson, R.A., 1999. The Donbas Foldbelt: its relationships with the uninverted Donets segment of the Dniepr–Donets Basin, Ukraine. Tectonophysics 313, 59–83.

Wagner, G.A., Van den haute, P., 1992. Fission-Track Dating. Enke Verlag, Stuttgart, Germany. 285pp.

Wolf, R.A., Farley, K.A., Kass, D.M., 1998. Modeling of the temperature sensitivity of the apatite (U–Th)/ He thermochronometer. Chem. Geol. 148, 105–114.

Zaun, P., Wagner, G.A., 1985. Fission track stability in zircon under geological conditions. Nucl.Tracks Radiat. Meas. 10, 303–307.

Ziegler, J.F., 1977. Helium: Stopping powers and ranges in all elemental matter. Pergamon, New York. 367 pp.